HHS Public Access

Author manuscript

J Tissue Eng Regen Med. Author manuscript; available in PMC 2019 July 13.

Published in final edited form as:

J Tissue Eng Regen Med. 2017 March ; 11(3): 658–668. doi:10.1002/term.1962.

Bioengineered post-natal recombinant tooth bud models

W. Zhang, **B. Vázquez**, and **P.C. Yelick***

Department of Oral and Maxillofacial Pathology, Tufts University, Boston, MA, USA

Abstract

The long-term goal of this study is to devise reliable methods to regenerate full-sized and fully functional biological teeth in humans. In this study, three-dimensional (3D) tissue engineering methods were used to characterize intact postnatal dental tissue recombinant constructs, and dental cell suspension recombinant constructs, as models for bioengineered tooth development. In contrast to studies using mouse embryonic dental tissues and cells, here the odontogenic potential of intact dental tissues and dental cell suspensions harvested from postnatal porcine teeth and human third molar wisdom tooth dental pulp were examined. The recombinant 3D tooth constructs were cultured in osteogenic media *in vitro* for 1 week before subcutaneous transplantation in athymic nude rat hosts for 1 month or 3 months. Subsequent analyses using X-ray, histological and immunohistochemical methods showed that the majority of the recombinant tooth structures formed calcified tissues, including osteodentin, dentin cementum, enamel and morphologically typical tooth crowns composed of dentin and enamel. The demonstrated formation of mineralized dental tissues and tooth crown structures from easily obtained post-natal dental tissues is an important step toward reaching the long-term goal of establishing robust and reliable models for human tooth regeneration.

Keywords

bioengineering; tooth bud; adult stem cells; tissue recombinants

1. Introduction

Many elegant studies have shown that tooth development and regeneration in mammals and other vertebrates is the result of tightly regulated, temporally and spatially controlled, interactions of the dental epithelium (DE) and the dental mesenchyme (DM) (Lumsden, 1988; Thesleff *et al.,* 1995; Thesleff and Jernvall, 1997). The odontogenic potential of developing mouse embryonic DE and DM tissues was determined using sophisticated tissue recombination techniques, which have since been established as powerful tools to analyse the tissue-specific inductive potential of a variety of tissues (Mina and Kollar, 1987). Using this approach, DE and DM tissues harvested from embryonic mouse tooth buds at discrete developmental stages were recombined with stage-matched and mismatched dental and non-

*Correspondence to: Pamela C. Yelick, Department of Oral and Maxillofacial Pathology, Division of Craniofacial and Molecular Genetics, Tufts University, Boston, MA 021111, USA. Pamela.yelick@tufts.edu.

Conflict of interest

The authors have declared that there is no conflict of interest.

dental tissues, and subsequently grown in culture. Analyses of these embryonic tissue recombinants showed that tooth formation resulted from recombinants of E9.5-E11.5 mouse DE combined with both CNC-derived DMand non-neural crest cells (NCC) derived mesenchyme (Mina and Kollar, 1987). After E11.5, odontogenic potential was demonstrated to reside with the DM, which was shown to direct ameloblast and odontoblast differentiation and tooth shape, when combined with both dental and non-dental epithelium (Kollar and Baird, 1970a,1970b; Thesleff *et al.,* 1977; Wolters and van Mullem, 1977; Kollar and Fisher, 1980). Furthermore, intact E10 mouse DE primordium was demonstrated to induce tooth formation when combined with dissociated cell suspensions consisting of mouse embryonic stem cells, neural stem cells and bone marrow cells (Ohazama *et al.,* 2004). Not only intact embryonic mouse dental tissues but also embryonic tooth bud-derived DE and DM cell suspensions also exhibited the potential to form complete teeth. Cell suspensions harvested from E14.5 mouse DE and DM tissues and seeded at high density into collagen droplets were shown to form fully functional teeth (Nakao *et al.,* 2007; Oshima *et al.,* 2011). A recent report also showed that adult human gingival epithelial cells, suspended in Cellmatrix type I and placed on mouse molar E14.5 DM and grown in the kidney capsule, also formed tooth-like structures, indicating the potential for E14.5 DM to induce both dental and non-dental epithelium to form dental epithelial derived enamel. In contrast, E17 mouse DM no longer exhibited the ability to induce tooth formation when combined with non-dental epithelium (Hata and Slavkin, 1978).

To date, the vast majority of successful tooth regeneration studies have been performed using embryonic mouse dental tissues and cells. Although extremely informative, these studies do not directly address the issue of human tooth regeneration, as autologous human embryonic tissues are not generally available for this purpose. To overcome this obstacle, this laboratory has pursued studies of postnatal dental tissues and cells for regenerative dental applications in humans. Previously published reports on dental tissue engineering showed that cells harvested from postnatal porcine and rat DE and DM also exhibit the capacity to form whole tooth crowns. It was demonstrated that DE and DM cells harvested from postnatal porcine and rat tooth buds, and seeded onto biodegradable polyester scaffolds, implanted *in vivo,* and grown for 12 weeks (rat) and 24 weeks (porcine), formed small tooth crowns that closely resembled those of naturally formed teeth (Young *et al.,* 2002; Duailibi *et al.,* 2004, 2008; Abukawa *et al.,* 2009). These provocative studies suggested the potential for clinically relevant tooth replacement therapies using cells harvested from human postnatal wisdom teeth – tissues that are normally discarded after extraction.

Published reports from many groups have shown that natural organ development can provide useful insight and guidance for the development of bioengineered organ models. These studies have shown that the establishment and maintenance of proper epithelial and mesenchymal cell interactions, which govern the development of all epidermal-derived organs, including teeth, whiskers, hair follicles, and mammary and salivary glands are of particular consideration and importance. (Lumsden, 1988; Hardy, 1992; Andl *et al.,* 2004; Ingman and Robertson, 2008). Therefore, establishing a robust bioengineered 3D tooth germ model that provides proper DE/DM cell interactions will also provide useful insight into a variety of bioengineered organ models (Thesleff *et al.,* 1977). The present study describes

characterizations of 3D bioengineered tooth bud models as templates for biological replacement tooth formation in humans.

2. Materials and methods

2.1. Porcine molar tooth bud isolation and preparation

All experiments involving the use of animals were reviewed and approved by the IACUC at Tufts University, Boston, MA, USA. The discarded mandibles of 6-month-old pigs were debrided of tissue and sanitized with 10% povidone iodine. Unerupted third molar (M3) and fourth molar (M4) tooth buds were carefully harvested from the prepared mandibles, and washed in Phosphate buffered saline (PBS) with 2% penicillin/streptomycin/amphotericin (PSA). Enamel and pulp organ tissues were carefully separated using surgical means, and any calcified tooth cusps were removed. Enamel and pulp organs harvested from M3 molar teeth were sectioned into four equal parts, while the smaller, less-developed M4 molar tooth enamel and pulp organs were split to two equal parts.

2.2. Cell isolation and culture

All cells were prepared as previously published (Young *et al.,* 2002). Briefly, harvested 6-month-old porcine M3 and M4 molar tooth buds were mechanically separated into enamel organ and pulp organ tissues. Healthy human gingiva and dental pulp tissues were harvested from extracted M3 wisdom teeth. All tissues were individually minced into < $1mm^3$ pieces, washed in PBS, enzymatically digested with 0.4 mg/ml type I collagenase (Sigma-AIdrich, St Louis, MO, USA) and 0.2 mg/ml Dispase I (Boehringer Mannheim, Indianapolis, IN, USA) in Hank's Balanced Salt Solution (HBSS) for 45 min at 37 °C, and gently dissociated by trituration. Cells were then washed and filtered using a sterile Falcon 40-micron cell strainer (Corning, Tewsbury, MA, USA) to generate single-cell suspensions. Porcine dental mesenchymal cells (pDM-C) and human dental pulp-derived mesenchymal cells (hDM-C) were expanded in Advanced Dulbecco's modified Eagle's Medium (DMEM)/F12 (12634; Life Technologies, Grand Island, NY, USA) with 10% fetal bovine serum (FBS), 25 μg/ml ascorbic acid, 1% Glutamax and 1% PSA. The pDE-C and human gingival epithelial cells (hGE-C) were expanded in LHC-8 (12678–017; Life Technologies) supplemented with 10% FBS with 0.5 μg/ml epinephrine and 1% PSA. All cells were expanded in culture and cryopreserved until use (~1 month), at which time the cells were expanded in the same media used for primary cell culture. The osteogenic potential of the hDM cells used in this study was first confirmed by demonstrating the formation of calcified nodules when cultured in osteogenic media.

2.3. Preparation of recombinant constructs

Four types of cell-loaded (C) collagen scaffold recombinant constructs and three types of intact tissue (T) recombinant constructs were prepared and examined (see Table 1) including: pDE-T + pDM-T, pDE-T + hDM-C, pDE-T + S, pDE-C + pDM-C, pDM-T + S, hGE-C + pDM-T and hGE-C + hDM-C. Twelve replicate samples were examined for each recombinant construct type, including six replicates implanted and grown for 1 month and six replicates implanted and grown for 3 months. Cell-loaded constructs consisted of 1.0×10^6 cells suspended in 50 p.1 of 1 mg/ml collagen type I (2.0×10^4 cells/μl), which were

either pipetted and cultured together, or pipetted onto tissue pieces, in individual 24-well plates. Constructs with collagen were gelled at 37 °C for 1 h before culture. All constructs were cultured in 1:1 (LHC-8:DMEM/F12) containing osteogenic supplements (10 mM β-glycerol phosphate, 100 nM dexamethasone and 50 μM ascorbic acid) and 1% PSA for 1 week before subcutaneous implantation.

2.4. *In vivo* subcutaneous implantations

All animal experiments were performed under the guidance and with the approval of the Tufts University Institutional Animal Care and Use Committee (IACUC). Replicate (12) recombinant constructs were implanted in a randomized fashion subcutaneously into 4-week-old nude rat hosts (RNU; Charles River, Wilmington, MA, USA). Six replicates, were implanted and grown for 1 month and six replicates were grown for 3 months. Host animals were killed by CO_2 asphyxiation followed by cervical dislocation. Harvested implants were examined by X-ray to detect calcified tissue formation, fixed in 4% formalin overnight at room temperature, washed with PBS, decalcified in a 1:1 solution of 45% formic acid–20% sodium citrate, processed and embedded in paraffin.

2.5. Histological and immunohistochemical (IHC) analyses of recombinant constructs

Paraffin-embedded samples were sectioned at 6 μm intervals. Selected sections were stained with haematoxylin and eosin (H&E), and analysed under bright field and polarized light microscopy (Zeiss, Axiophot Imager; Göttingen, Germany). Immunohistochemical analyses were performed on selected sections of each construct using the bone-specific anti-body for osteocalcin (OC, 1:80 dilution, ab13418; Abcam, Cambridge, MA, USA), the dental enamel tissue specific antibody for amelogenin (AM, 1:8 000 dilution; kind gift of Dr Jim Simmer) and the dentin-specific antibody for dentin sialophosphoprotein (DSPP, 1:4,000 dilution; kind gift of Dr Larry Fisher). For IHC, all sections were incubated with biotinylated secondary antibody, stained using the Vectastain ABC staining kit (Vector Laboratories, Burlingame, CA, USA) and counterstained with Fast Green (Sigma-Aldrich, St. Louis, MO, USA). Processed sections were dehydrated through a graded ethanol series, sealed with Permount (Thermo Fisher Scientific Inc., Fair Lawn, NJ, USA), and analysed using Zeiss Axiophot and M2Bio microscopes. Photographs were obtained by digital Zeiss Axiocam camera, and manipulated using Adobe Photoshop.

3. Results

The experimental strategy was to create post-natal recombinant dental constructs consisting of various combinations of porcine and human post-natal tissues and cells (Figure 1). Owing to the prohibitively large number of samples that would need to be generated and analysed if every possible combination were examined, we carefully selected the following seven recombinant constructs for this study: pDE-T + pDM-T, pDE-T + hDM-C, pDE-T + S, pDE-C + pDM-C, pDM-T + S, hGE-C + pDM-T and hGE-C + hDM-C (Figure 1).

The porcine mandibular M3 tooth buds used in this study were late differentiation stage, exhibiting dental papilla and enamel organ tissues fully separated by tooth cusps (Figure 2A–C). The M3 molar dental papilla (DP) tissues appeared pale in colour (Figure 2C), and

were much stiffer than human molar dental pulp tissues. In contrast, porcine M3 enamel organ (EO) tissues were soft in texture, and highly vascularized (Figure 2C). Porcine M4 molar tooth buds were less developed, smaller and softer than M3 tooth buds, and contained only partially calcified tooth cusps (Figure 2D and F, respectively). M4 molar teeth also appeared less vascularized than M3 tooth buds by visual inspection (Figure 2, Panel B vs. D). Both M3 and M4 molar DP and EO tissues were easily separated, minimizing the potential for DE and DM tissue cross-contamination. Cryopreserved cells generated from 6-month-old porcine M3 and M4 molar DE and DM tissues were thawed and expanded as described previously (Young *et al.,* 2002). Human dental pulp and human gingival epithelium were harvested from extracted healthy wisdom teeth and used to generate single-cell suspensions that were expanded in culture. Cryopreserved, thawed and cultured pDE, pDM, hDM and hGE cells exhibited similar behaviours as their corresponding primary cell cultures. Porcine DE and hGE cells exhibited typical cobblestone epithelial cell morphology, while pDM and hDM cells exhibited typical spindle shape mesenchymal cell morphology (Figure 3A–D).

3.1. Recombinant constructs after 1week culture in osteogenic media

Before subcutaneous implantation in nude rat hosts, 12 replicates of each of the seven types of postnatal recombinant constructs were cultured *in vitro* for 1week in osteogenic media. Bright field microscopic analyses of the recombinants after 1week of culture in osteogenic media revealed distinct cell growth and calcified nodule formation in several of the constructs (Figure 3G,I–L). The pDE-C + pDM-C constructs exhibited the most distinct mineralized tissue formation (Figure 3I, arrows). In addition, robust cell outgrowth was observed in all recombinant constructs except for the pDE-T + pDM-T and pDE-T + S recombinant constructs (Figure 3E,F).

3.2. *In vivo* implantation and harvesting of recombinant constructs

At the time of sample collection, all of the implants were easily located and separated from surrounding host tissue (Figure 4A, arrows). Sutures used to sew tissue constructs together were easily identifiable in 1-month implants but were not detectable and had presumably been resorbed in 3-month implants. Radio-opaque calcified tissue formation was visible by X-ray in some of the recombinant implants (Figure 4B,C).

3.3. Histological analyses

Histological analyses of paraffin embedded and sectioned recombinant constructs were used to examine soft and mineralized tissue formation in each type of postnatal recombinant construct. Microscopic examination revealed distinct mineralized tissue formation in a variety of constructs, including bone, osteodentin, dentin, enamel and cementum. Correlation of postnatal recombinant construct type with the types of mineralized tissues detectable in each type of construct 1 month and 3 months after subcutaneous implantation are shown in Table 1 and described below.

The most consistent and robust mineralized tissue formation was observed in the pDE-T + pDM-T recombinant constructs, which exhibited mineralized tissue formation in 9/12 (75%)

of the implants, including 6/6 replicates 1 month after implantation, and 3/6 replicates 3 months after implantation (Figure 5A,A',B,B').

The second highest percentage of mineralized tissue formation was observed in two different postnatal recombinant construct types, namely the pDE-T + hDM-C, and pDE-T + S recombinant constructs. Both the pDE-T + hDM-C, and the pDE-T + S recombinant constructs formed mineralized tissues in 50% (6/12) of the implants (Figure 5C–F,C'–F'). For the pDE-T + hDM-C construct, 4/6 (66.7%) exhibited mineralized tissue formation 1 month after implantation, while 2/6 (33.3%) exhibited mineralized tissue formation 3 months after implantation (Figure 5C,C',D,D'). For the pDE-T + S constructs, 2/6 (33.3%) formed mineralized tissues after 1 month, and 4/6 (66.7%) after 3 months (Figure 5E,E',F,F').

The next highest percent mineralization was observed in the pDE-C + pDM-C recombinant constructs, which exhibited small areas of bone-like tissue in 2/6 (33%) of the 3-month implants and in none (0/6) of the 1-month implants (total 2/12 = 16.7%) (Figure 5H,H',I,I').

The two types of hGE-C-containing constructs, hGE-C + hDM-C and pDM-T + hGE-C, both exhibited mineralized tissue formation in only 1/12 (8%) of the constructs, in only one of the 3-month implants and in none of the 6-month implants (Figure 5J–M,J'–M'). Lastly, no calcified tissue formation was observed in any of the pDM-T + S recombinants (0/12, 0%) either 1 month or 3 months after implantation (Figure 5N,N',O,O'). These results demonstrated that under these experimental conditions, postnatal pDM-T alone is not competent to form dentin, cementum or alveolar bone while, in contrast, constructs consisting of pDM-T combined with pDE-T formed mineralized tissues in 9/12 (75%) of the implants (Table 1 and Figure 5).

Which post-natal recombinant constructs exhibited the ability to form whole tooth crown structures were evaluated next. Typical tooth crown-like structures consisting of both enamel and dentin were present in the following four types of postnatal recombinant constructs: those containing pDE-T in combination with either pDM-T (1/12, 8%), hDM-C (1/12, 8%) or acellular collagen (S) (1/12, 8%), and in one recombinant construct sample consisting of pDE-C + pDM-C (1/12,8%). These results demonstrated that intact postnatal DE tissue, and cultured DE cells resuspended in collagen gel, when combined with postnatal DM tissues and cells exhibit the capacity to from tooth crowns (Figure 5A,D). Surprisingly, pDE-T combined with acellular collagen scaffold (S) alone also formed tooth crowns in 1/12 implants, suggesting the possible recruitment of host mesenchymal cells to participate in tooth crown formation.

It is also noteworthy that the size of the tooth crowns that formed in the postnatal recombinant tooth bud constructs evaluated in this study were quite large (~5 mm high and 3 mm wide) compared with those previously generated using PGA/PLGA scaffolds (~50 μm diameter; Young *et al.,* 2002). No obvious differences were observed in the quality of the mineralized dental tissues formed using M3 or M4 molar tissues.

3.4. Immunohistochemical and immunofluorescent (IF) analyses

The IHC analyses revealed that most of the bone and osteodentin-like calcified tissues present in recombinant constructs expressed both osteocalcin (OC) and dentin sialophosphoprotein (DSPP) (Figure 6A,A' and B,B', respectively). Bioengineered dentin–pulp complex structures exhibited DSPP expression in odontoblasts, dentin and enamel (Figure 6C,C') and amelogenin (AM) expression in bioengineered enamel (Figure 6D,D').

It is noteworthy that demineralized bioengineered enamel appeared similar to naturally formed demineralized enamel matrix (Figure 7B,B'). Another observation is that all of the recombinant constructs fabricated from M3 pDM-T exhibited centrally located necrotic tissue after 1 month of implantation, while only 3/24 (12.5%) of the less mature M4 pDM-T-containing recombinant constructs exhibited a small amount of necrotic tissue at 3 months, along with small areas of calcified tissue formation at the periphery of the necrotic tissues (Figure 7G). Also of interest is the fact that some of the constructs containing hGE-C formed mucosa-like structures consisting of polarized epithelial cell tissue layers (Figure 5N,N').

To summarize, four types of calcified tissue were found in the implants: (1) bone/osteodentin, (2) dentin, (3) enamel and (4) acellular cementum. Most of the calcified tissues appeared to be alveolar bone or osteodentin-like tissues, mainly consisting of spongy bone tissue containing trabecular bone of various sizes and shapes, and bone marrow-like tissue (Figure 7A,A',A"). Recombinant dentin, enamel and acellular cementum all exhibited the typical morphologies observed in naturally formed teeth (Figure 7B,B',B").

Certain recombinant construct bioengineered tooth crowns consisted of well-organized enamel matrix aligned alongside dentin with clear tubular structures (Figure 7B), while others exhibited atypical and dysmorphic tooth crowns, with enamel tissues surrounded by dentin (Figure 7F). The formation of sandwiched enamel–dentin–enamel structures, were observed in pDE-T + S recombinant constructs. The extracellular matrix of the calcified tissue closely resembling acellular cementum appeared tightly woven (Figure 7C,C',C"). Acellular cementum-like tissue formation was only detected in samples containing pDM-T.

4. Discussion

Tissue engineering designs that mimic natural organ and tissue development have been shown to be successful for bioengineered tissue and organ regeneration (2000). Based on this strategy, postnatal dental and non-dental tissue, and cell recombinants as 3D models for human tooth regeneration have been characterized. In natural tooth development, DE and DM tissue interactions are regulated by over 300 genes and 100 growth and differentiation factors, which act concertedly in a strict temporal and spatial manner to induced dental cell differentiation and tooth morphogenesis (Jernvall and Thesleff, 2000). During the early stages of tooth development, dental epithelial and ectomesenchymal tissues that formed the further dental tissues are separated by a thin layer of basement membrane(Veis, 2003). Only the DE and DM cells aligned along the basement membrane can differentiate into enamel-forming ameloblasts and dentin-forming odontoblasts. Unlike the other dental-related tissues, the main components of basement membrane are collagen IV (Nagai *et al.,* 2001;

Poschl *et al.,* 2004). Tissue engineering approaches that provide localized environments that mimic the features of natural tooth development and are conducive to proper DE/DM cell interactions, will support tissue differentiation and tooth development. Furthermore, based on the importance of the scaffold for proper mechanical cues, optimized scaffolding material should provide enough mechanical strength to support the formation of the regenerated tissues, while at the same time exhibit degradation rates that closely match that of new dental tissue formation.

The results obtained in this study demonstrate that in some cases, mechanically separated intact postnatal DE and DM tissues, and cultured postnatal DE and DM cell suspensions, retain the ability to differentiate into dental tissues and mature tooth crowns. These results expand upon previously published reports of embryonic mouse recombinant DE and DM tissue constructs and are consistent with previously published tooth tissue engineering studies, which showed that mixed populations of post-natal porcine and rat DE and DM cells exhibited the capacity to form small, morphologically correct tooth crowns (Young et *al.,* 2002).

The fact that not all of the replicate postnatal dental tissue and cell recombinants examined in this study resulted in mineralized tissue formation indicates that additional attention must be made with respect to the design of reliable and robust models for human tooth regeneration. For example, we found that porcine dental DE and DM cells encapsulated in collagen were not as consistent in forming tooth crowns compared with intact pDE/pDM tissue recombinants, likely indicating insufficient DE-DM cell contact and cross-talk in the collagen gel dental cell suspension constructs. In addition, recombined pDE-T and pDM-T constructs exhibited a 4–5 day developmental delay compared with intact (non-dissociated) tooth buds, further emphasizing the importance of direct physiological contact between the dental epithelium and mesenchyme for successful tooth formation (Cummings et al., 1981). Previously published reports that mixed suspensions of cultured post-natal porcine and rat DE and DM cells that were seeded directly onto PLGA scaffolds were able to form small, organized tooth structures, suggest that when grown in close proximity (without collagen), post-natal DE and DM cells can reorganize themselves to form small tooth crowns (Young *et al.*, 2002, 2005; Duailibi *et al.,* 2004). A feature common to all the previous models used for tooth crown formation is that they allowed for direct contact between DE and DM cells. It is possible that the cell seeding density used to seed the collagen scaffold did not provide the critical DE–DM cell–cell contact and cross-talk necessary to support tooth crown formation. Similarly, although the osteogenic differentiation potential of the human dental pulp-derived DM cells used in this study was validated by two-dimensional *in vitro* culture, hDM cells did not exhibit robust mineralized dental tissue in 3D culture in collagen gel. Again, this result suggests that the cell seeding density used in this type I collagen 3D tooth model did not allow for optimized DE–DM cell signalling required for whole-tooth tissue engineering, and indicate the need for further evaluation of alternative approaches.

While human dental pulp-derived DM cells can be harvested from extracted wisdom teeth, one of the main obstacles for research on human tooth regeneration is the lack of availability of competent human DE cells. It has been reported that adult human gingival epithelial cells pipetted directly onto E14.5 mouse molar tooth dental mesenchyme within a Celmatrix type

I-A gel droplet, cultured for 5 days, and grown in a kidney capsule for 6 weeks, formed small tooth structures (Angelova Volponi *et al.,* 2013). This report suggests that the fact that the human GE constructs in the present study did not induce tooth formation may either reflect the competency of the DM tissues used in the two studies (E14.5 vs. post-natal), or may also reflect insufficient direct contact with DM cells or tissues used in the present study. We will further examine these possibilities in future studies.

It has been reported that transplanted neonatal dental pulp tissue containing residual DE cells developed into tooth-like structures consisting of mineralized tubular dentin, predentin and a vascularized pulp-like chamber lined with functional odontoblast-like cells, although no enamel formation was observed (Lyaruu *et al.,* 1999). In the present study, tubular dentin formed adjacent to enamel tissue in all samples containing pDE tissue, and in one construct generated from pDE and pDM cells. These results suggest that postnatal porcine enamel organ tissue and cells retain the potential to guide tooth formation.

Necrotic tissue was observed in all samples containing M3 DM tissue, but not in samples containing M4 DM tissue. This may reflect the fact that the vasculature is less developed in the less mature M4 molar tooth buds, which can allow these constructs to be more easily integrated with the host vasculature, as compared with M3 DM tissues which contain more developed vasculature. M3 molar DM tissues are also much stiffer than the M4 molar DM tissues, which could also interfere with efficient host vasculature invasion and infiltration, and corresponding oxygen and nutrient exchange. Inadequate blood supply in M3 DM tissue implants would in turn hinder dental stem cell differentiation, based on the fact that the highly vascularized nature of dental tissues is thought to be indispensable for proper maturation and mineralization (Baba *et al.,* 1996).

Although DE and DM tissues of porcine M3 and M4 were very easily separable, allowing for clean sample preparation of harvested DE and DM tissues, it is possible that small remnants of contaminating DM and DE tissues remained in isolated DE and DM tissue, respectively. The presence of small amounts of DM tissue remaining in the isolated DE tissue sample could explain the ability for DE-T recombined with acellular collagen scaffold (S) to form DM cell-derived osteodentin and bone at similar efficiencies, as observed in DE-T + collagen encapsulated DM cell constructs. Another more exciting possibility is that pDE-T was able to recruit rat host cells to participate in DM-cell-derived dental tissue formation. Future studies using lineage traced cell lines and animal hosts will be used to investigate this exciting possibility.

Comparison of mineralized tissue formation in 1-month and 3-month implants was somewhat surprising. Although it was anticipated that 3-month implanted recombinant constructs would exhibit similar or more robust dental tissue formation compared with 1-month samples, this was not the case. This observation is likely a result of the relatively small sample size (six 1-month and six 3-month replicate constructs) used in this study, and will be further examined in future experiments

5. Conclusions

In conclusion, the present study demonstrated the following important points. Full-sized bioengineered 3D tooth buds generated from postnatal tissues and cells can be used to form mineralized dentin, enamel and whole tooth crowns, demonstrating the potential utility of postnatal dental tissues for human tooth regeneration. Recombinant constructs consisting of intact porcine DE and DM tissues from postnatal M3 and M4 teeth, comparable in developmental stage to that of human wisdom teeth, were capable of forming mineralized tissues. These results support the promising utilization of postnatal dental tissues for regenerative tooth tissue engineering approaches in humans. In addition, recombinant porcine M3 and M4 DE tissue retained the potential to form complete tooth crowns when combined with intact pDM tissue, with pDM cells resuspended in collagen and with acellular collagen scaffolds alone. The fact that pDE tissue recombined with acellular collagen scaffold formed complete tooth crowns suggests the exciting possibility of adult host cell homing and recruitment for DM cell-derived tissue regeneration, although additional future studies are needed to confirm this possibility.

The results of the present study show that, when available, human postnatal DE harvested from extracted wisdom teeth may be a convenient and appropriate DE tissue for human tooth regeneration. Human third molar wisdom teeth, the last teeth to mature, begin calcification at approximately 8–10 years of age and complete tooth crown development between 12 and 16 years of age. Thus, it may be possible to harvest human third molar wisdom teeth at early developmental stages similar to those of the porcine M3 and M4 molar teeth used in the present study, to use in regenerative tooth applications in humans.

Together, the results obtained from this postnatal dental tissue recombinant study are promising for the eventual development of effective methods for tooth regeneration in humans. These and future studies continue to inform efforts to bioengineer functional biological replacement tooth buds for regenerative medicine applications in humans.

Acknowledgements

The authors would like to thank the members of the Yelick Laboratory for their critical expert advice on the results presented in this report. This work was supported by NIH/NIDCR R01 DE016132 (PCY).

References

2000; Tissue engineering. Nat Biotechnol 18 (suppl): It56–It58. [PubMed: 11221720]

Abukawa H, Zhang W, Young CS, et al. 2009; Reconstructing mandibular defects using autologous tissue-engineered tooth and bone constructs. J Oral Maxillofac Surg 67: 335–347. [PubMed: 19138608]

Andl T, Ahn K, Kairo A, et al. 2004; Epithelial bmpr1a regulates differentiation and proliferation in postnatal hair follicles and is essential for tooth development. Development 131: 2257–2268. [PubMed: 15102710]

Angelova Volponi A, Kawasaki M, Sharpe PT. 2013; Adult human gingival epithelial cells as a source for whole-tooth bioengineering. J Dent Res 92: 329–334. [PubMed: 23458883]

Baba T, Terashima T, Oida S, Sasaki S. 1996; Determination of enamel protein synthesized by recombined mouse molar tooth germs in organ culture. Arch Oral Biol 41: 215–219. [PubMed: 8712977]

Cummings EG, Bringas PJR, Grodin MS, et al. 1981; Epithelial-directed mesenchyme differentiation in vitro model of murine odontoblast differentiation mediated by quail epithelia. Differentiation 20: 1–9. [PubMed: 7308607]

Duailibi MT, Duailibi SE, Young CS, et al. 2004; Bioengineered teeth from cultured rat tooth bud cells. J Dent Res 83: 523–538. [PubMed: 15218040]

Duailibi SE, Duailibi MT, Zhang W, et al. 2008; Bioengineered dental tissues grown in the rat jaw. J Dent Res 87: 745–750. [PubMed: 18650546]

Hardy MH. 1992; The secret life of the hair follicle. Trends Genet 8: 55–61. [PubMed: 1566372]

Hata RI, Slavkin HC 1978; de novo induction of a gene product during heterologous epithelial – mesenchymal interactions in vitro. Proc Natl Acad Sci USA 75: 2790–2794. [PubMed: 275848]

Ingman WV, Robertson SA. 2008; Mammary gland development in transforming growth factor beta1 null mutant mice: systemic and epithelial effects. Biol Reprod 79: 711–717. [PubMed: 18614704]

Jernvall J, Thesleff I. 2000; Reiterative signaling and patterning during mammalian tooth morphogenesis. Mech Dev 92: 19–29. [PubMed: 10704885]

Kollar EJ, Baird GR. 1970a; Tissue interactions in embryonic mouse tooth germs. I. Reorganization of the dental epithelium during tooth-germ reconstruction. J Embryol Exp Morphol 24: 159–171. [PubMed: 5487154]

Kollar EJ, Baird GR. 1970b; Tissue interactions in embryonic mouse tooth germs. II. The inductive role of the dental papilla. J Embryol Exp Morphol 24: 173–186. [PubMed: 5487155]

Kollar EJ, Fisher C. 1980; Tooth induction in chick epithelium: expression of quiescent genes for enamel synthesis. Science 207: 993–995. [PubMed: 7352302]

Lumsden AG. 1988; Spatial organization of the epithelium and the role of neural crest cells in the initiation of the mammalian tooth germ. Development 103(Suppl): 155–169. [PubMed: 3250849]

Lyaruu DM, van Croonenburg EJ, van Duin MA, et al. 1999; Development of transplanted pulp tissue containing epithelial sheath into a tooth-like structure. J Oral Pathol Med 28: 293–296. [PubMed: 10432194]

Mina M, Kollar EJ. 1987; The induction of odontogenesis in non-dental mesenchyme combined with early murine mandibular arch epithelium. Arch Oral Biol 32: 123–127. [PubMed: 3478009]

Nagai N, Nakano K, Sado Y, et al. 2001; Localization of type IV collagen a 1 to a 6 chains in basement membrane during mouse molar germ development. Int J Dev Biol 45: 827–831. [PubMed: 11732842]

Nakao K, Morita R, Saji Y, et al. 2007 The development of a bioengineered organ germ method. Nat Methods 4: 227–230. [PubMed: 17322892]

Ohazama A, Modino SA, et al. 2004; Stem-cell-based tissue engineering of murine teeth. J Dent Res 83: 518–522. [PubMed: 15218039]

Oshima M, Mizuno M, Imamura A, et al. 2011; Functional tooth regeneration using a bioengineered tooth unit as a mature organ replacement regenerative therapy. Plos One 6: e21531.

Poschl E, Schlotzer-Schrehardt U, Brachvogel B, et al. 2004; Collagen IV is essential for basement membrane stability but dispensable for initiation of its assembly during early development. Development 131: 1619–1628. [PubMed: 14998921]

Thesleff I, Jernvall J. 1997; The enamel knot: a putative signaling center regulating tooth development. Cold Spring Harb Symp Quant Biol 62: 257–267. [PubMed: 9598359]

Thesleff I, Lehtonen E, Wartiovaara J, Saxen L. 1977; Interference of tooth differentiation with interposed filters. Dev Biol 58: 197–203. [PubMed: 873058]

Thesleff I, Vaahtokari A, Kettunen P, et al. 1995; Epithelial-mesenchymal signaling during tooth development. Connect Tissue Res 32: 9–15. [PubMed: 7554939]

Veis A 2003; Amelogenin gene splice products: potential signaling molecules. Cell Mol Life Sci 60: 38–55. [PubMed: 12613657]

Wolters JM, van Mullem PJ. 1977 Electron microscopy of epithelio-mesenchyme intercellular communication in trans-filter cultures of rat tooth germs. Arch Oral Biol 22:705–709. [PubMed: 272144]

Young CS, Terada S, Vacanti JP, et al. 2002; Tissue engineering of complex tooth structures on biodegradable polymer scaffolds. J Dent Res 81: 695–700. [PubMed: 12351668]

Young CS, Abukawa H, Asrican R, et al. 2005; Tissue-engineered hybrid tooth and bone. Tissue Eng 11: 1599–610. [PubMed: 16259613]

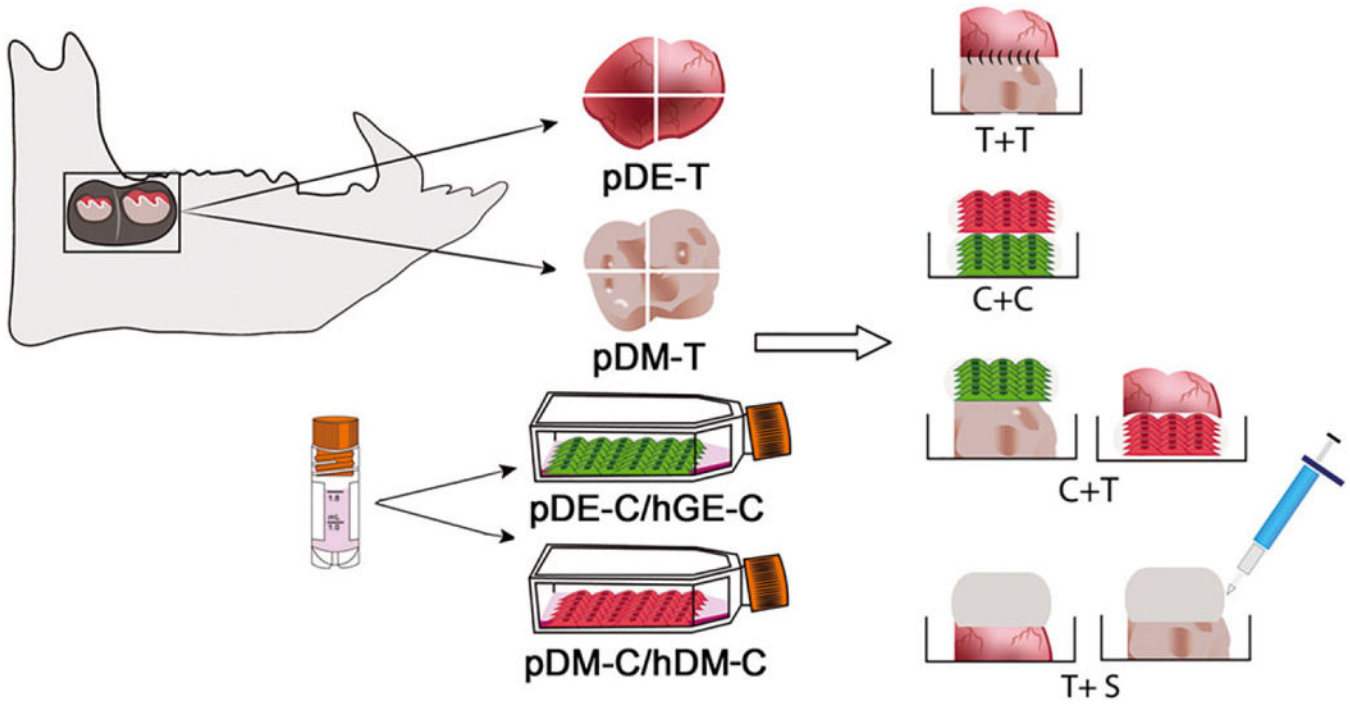

Figure 1.

Schematic representation of bioengineered recombinant tooth bud construct fabrication. Postnatal dental recombinant constructs were fabricated from M3 and M4 molar porcine dental epithelium (DE) and differentiation medium (DM) tissues (pDE-T, pDM-T), human dental pulp tissues and cells (hDM-T and hDM-C), and human gingival epithelial cell suspensions (hGE-C) as indicated. Tissue-tissue (T + T) recombinant constructs were sutured together, while cultured cells were resuspended in collagen and pipetted over tooth tissues to generate C + T constructs, or layered together to generate the cell-cell (C + C) constructs. Dental tissues layered with acellular collagen scaffold (S) were used as tissue alone controls.

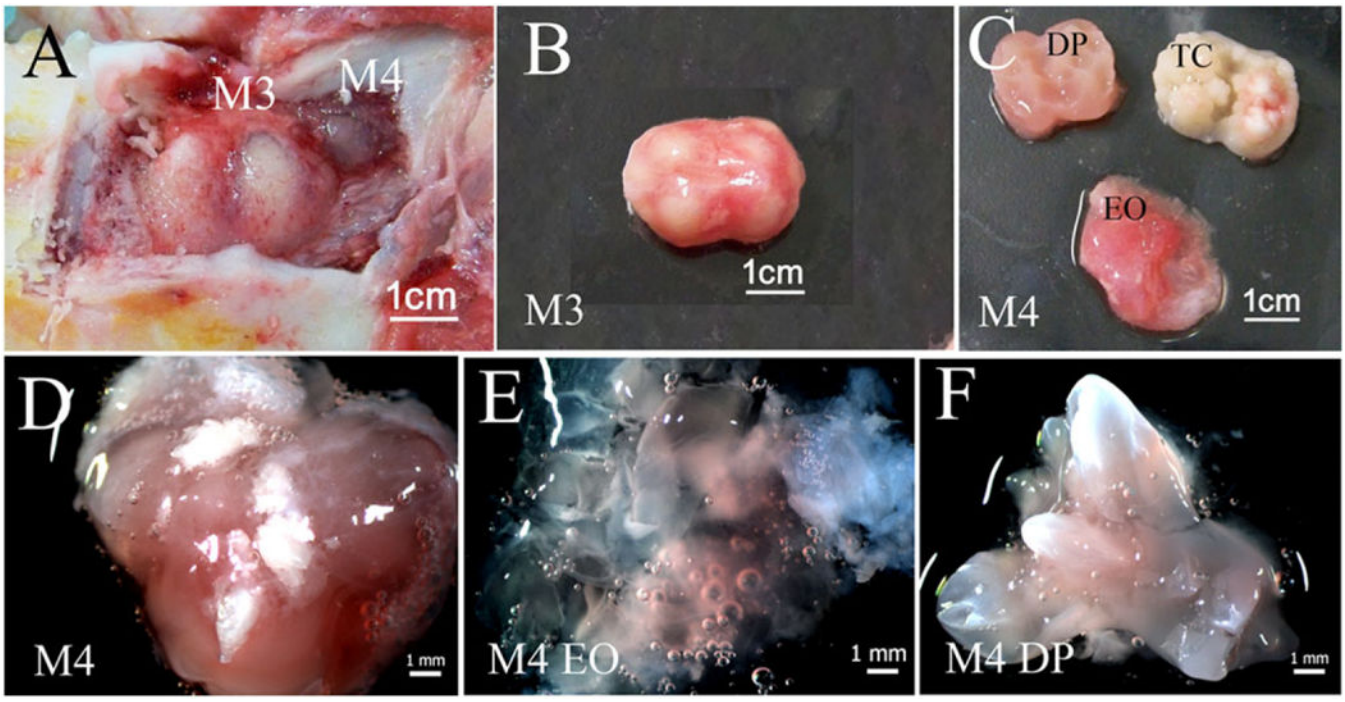

Figure 2.

Tooth bud isolation: (A) Exposed 6-month-old porcine mandibular M3 and M4 molar tooth buds in the jaw; (B) an isolated M3 tooth bud; (C) an M3 molar tooth bud dissected into enamel organ tissue (EO), calcified tooth cusps (TC) and dental papilla (DP) tissue; (D) an intact M4 molar tooth bud; (E) dissected M4 molar tooth EO; (F) DP tissues.

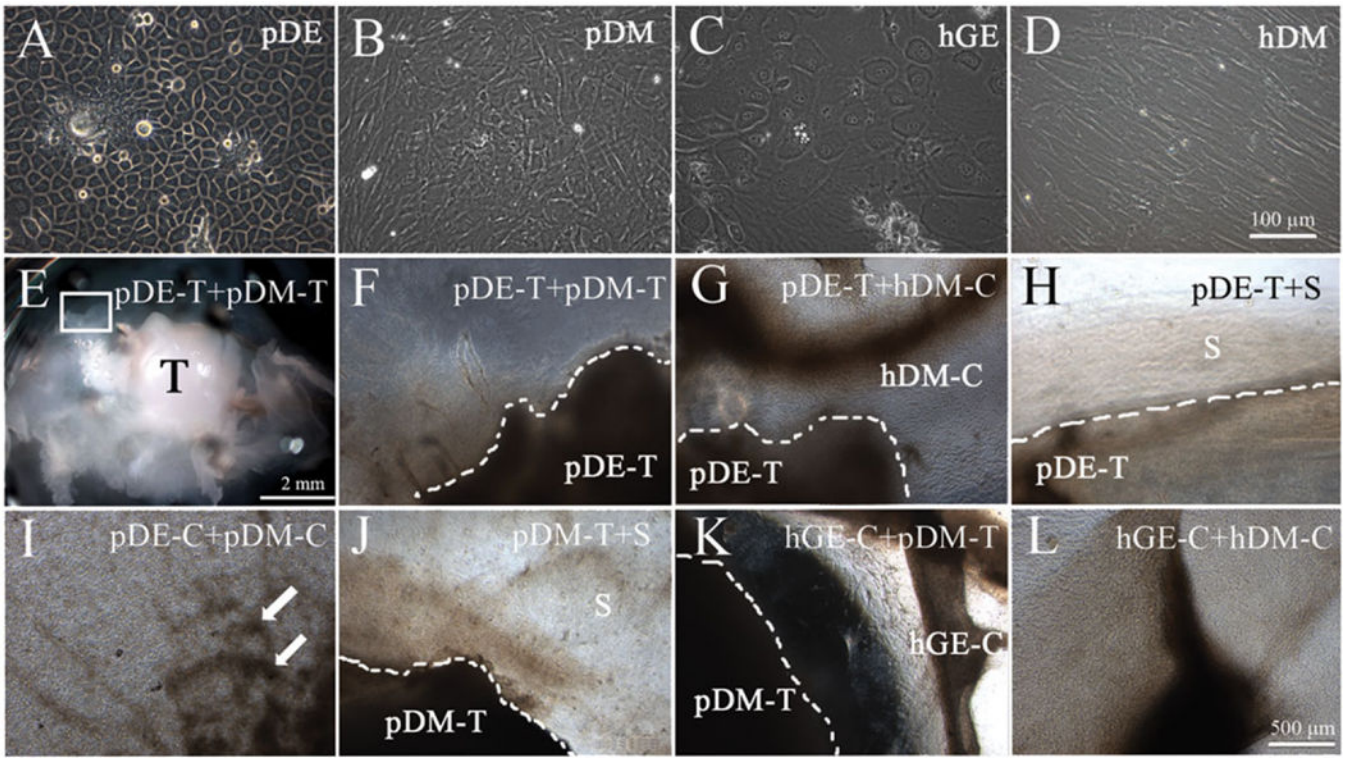

Figure 3.

In vitro cultured recombinant constructs. Cultured porcine dental epithelial (pDE) (A) and human gingival epithelial (hGE) cells (C) exhibited typical cobblestone epithelial cell morphology, while porcine dental mesenchymal (pDM) (B) and human dental mesenchymal (hDM cells) (D) exhibited typical spindle-shaped mesenchymal cell morphology. Bright field images of recombinant constructs, as labelled, cultured *in vitro* for 1 week in osteogenic media (E–H). White arrows indicate mineralized nodule formation. Scale bars: A–D, 100 μm; E, 2 mm; G–L, 500 μm.

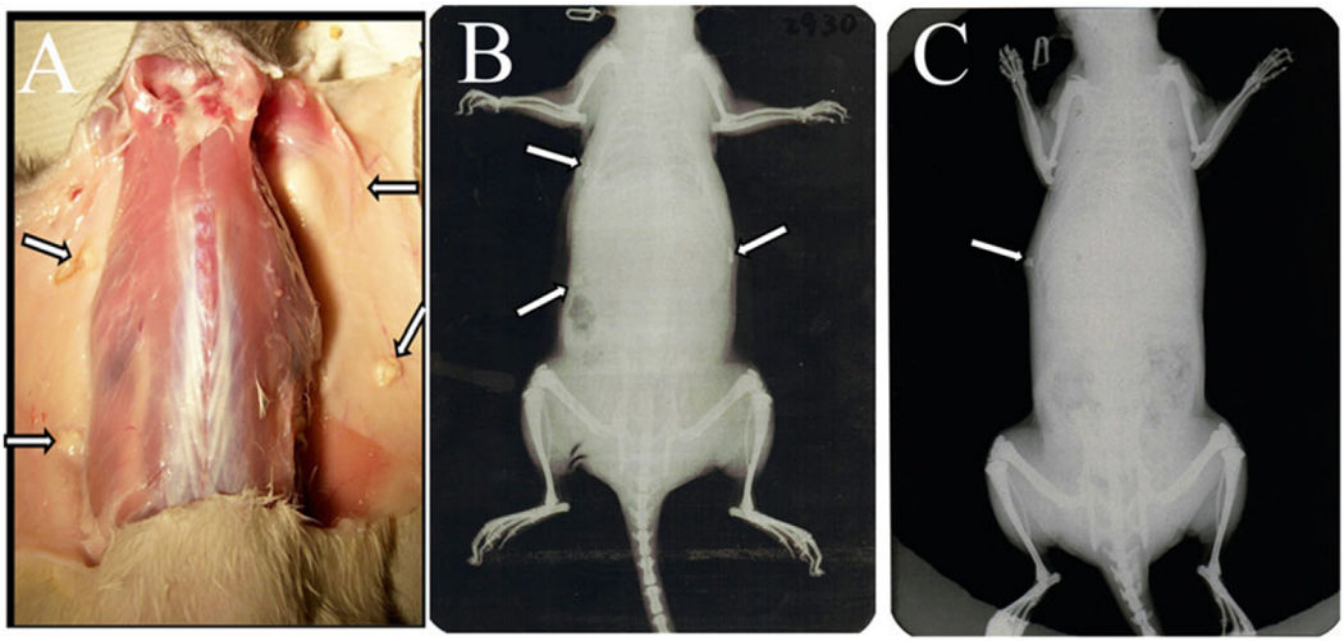

Figure 4.

Harvesting subcutaneous recombinant postnatal tooth constructs. (A) Recombinant constructs harvested at 1 month. Arrows indicate the location of each of four implants. X-ray imaging at 1 month (B) and 3 months (C) revealed calcified tissue formation (arrows).

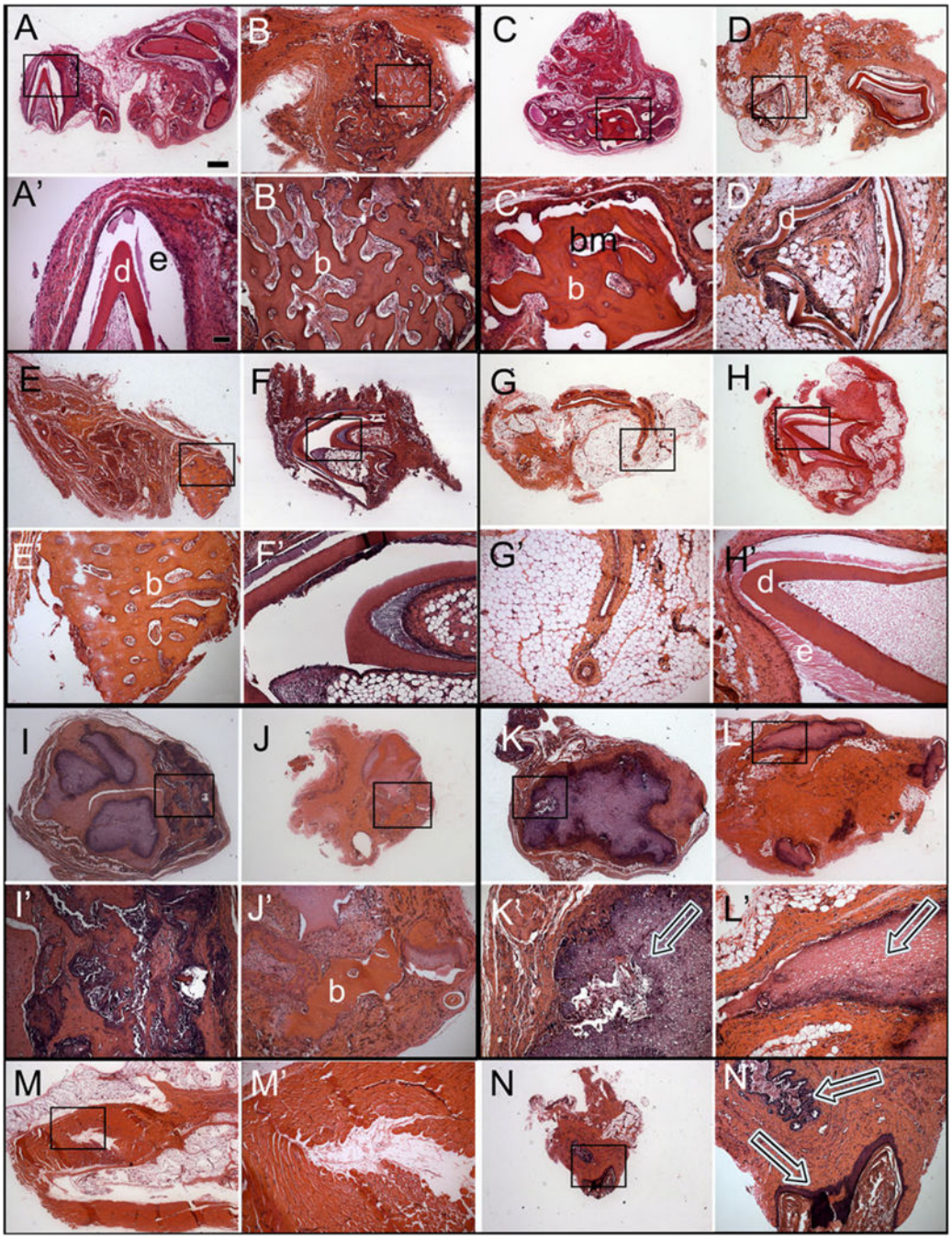

Figure 5.

Histological analyses of subcutaneous post-natal recombinant constructs. Haematoxylin and eosin (H&E) stained paraffin embedded and sectioned implants. Letter panels with primes represent higher magnification images of the boxed regions of each corresponding lettered panel. (A,A') Cusp formation in a pDE-T + pDM-T sample harvested after 1 month. (B,B') Bone/osteodentin-like tissue in a pDE-T + pDM-T sample after 3 months. (C,C') Bone/osteodentin-like tissue in a pDE-T + hDM sample after 1 month. (D,D') Cusp formation in a pDE-T + hDM sample after 3 months. (E,E') Bone/osteodentin-like tissue in a pDE-T + S

sample after 1 month. (F,F') Cusp formation in a pDE-T + S sample after 3 months. No calcified tissue was found in pDE-C + pDM-C samples at 1 month (G), and only in one implant at 3 months (H). Bone/osteodentin-like tissue present in hGE-C + pDE-T samples at 1 month (I) and 3 months (J). (K,L) Necrotic DM tissue was observed in most pDM-T + S implants at 1 month (K) and 3 months (L) (arrows). (M,N) Most hGE-C + hDM-C implants showed no sign of calcification (M), but contained mucosal epithelial-like tissues (N). hDM-C, human dental pulp derived dental mesenchymal cells; pDE-T, porcine dental epithelial tissue; pDM-T, porcine dental mesenchymal tissue; S, acellular collagen scaffold. Scale bars: A–N, 500 μm; A'-N', 50 μm.

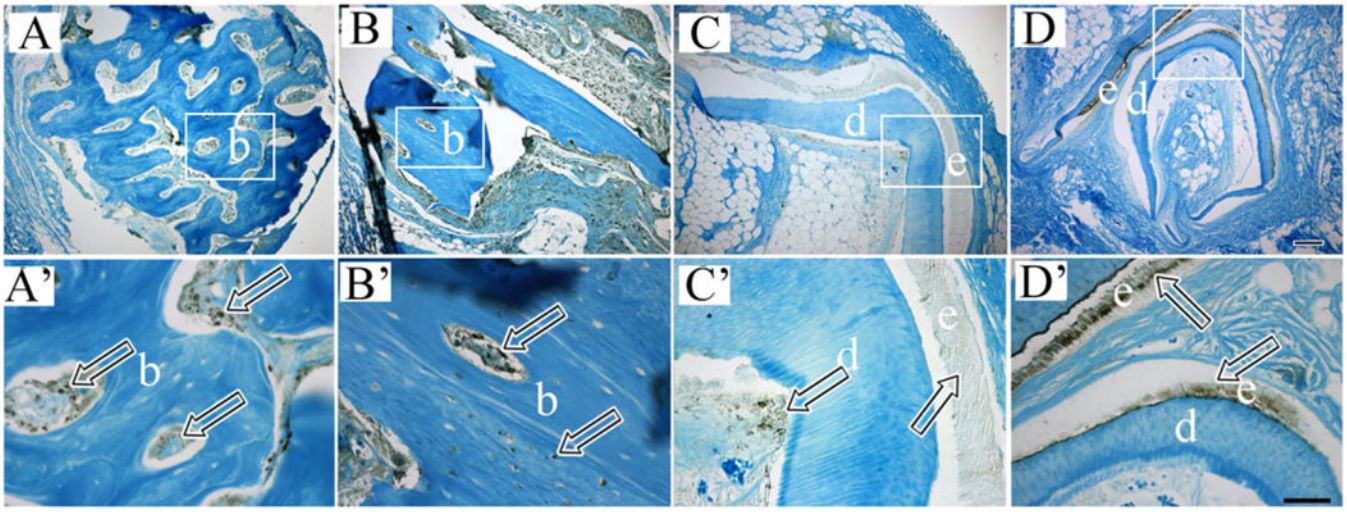

Figure 6.

Immunohistochemical analyses of bioengineered dental tissues. Primed letter panels show higher magnification images of boxed regions in corresponding letter panels. Bioengineered dentin/osteodentin-like tissues exhibited positive staining for osteocalcin (OC) (A and A', arrows) and dentin sialophosphoprotein (DSPP) (B and B', arrows). Bioengineered dentin and enamel-like tissues exhibited positive staining for DSPP (C and C', arrows), and bioengineered enamel tissues exhibited positive staining for amelogenin (AM) (D and D'. arrows). Scale bars: A–D, 500 m; A'–D', 50 m.

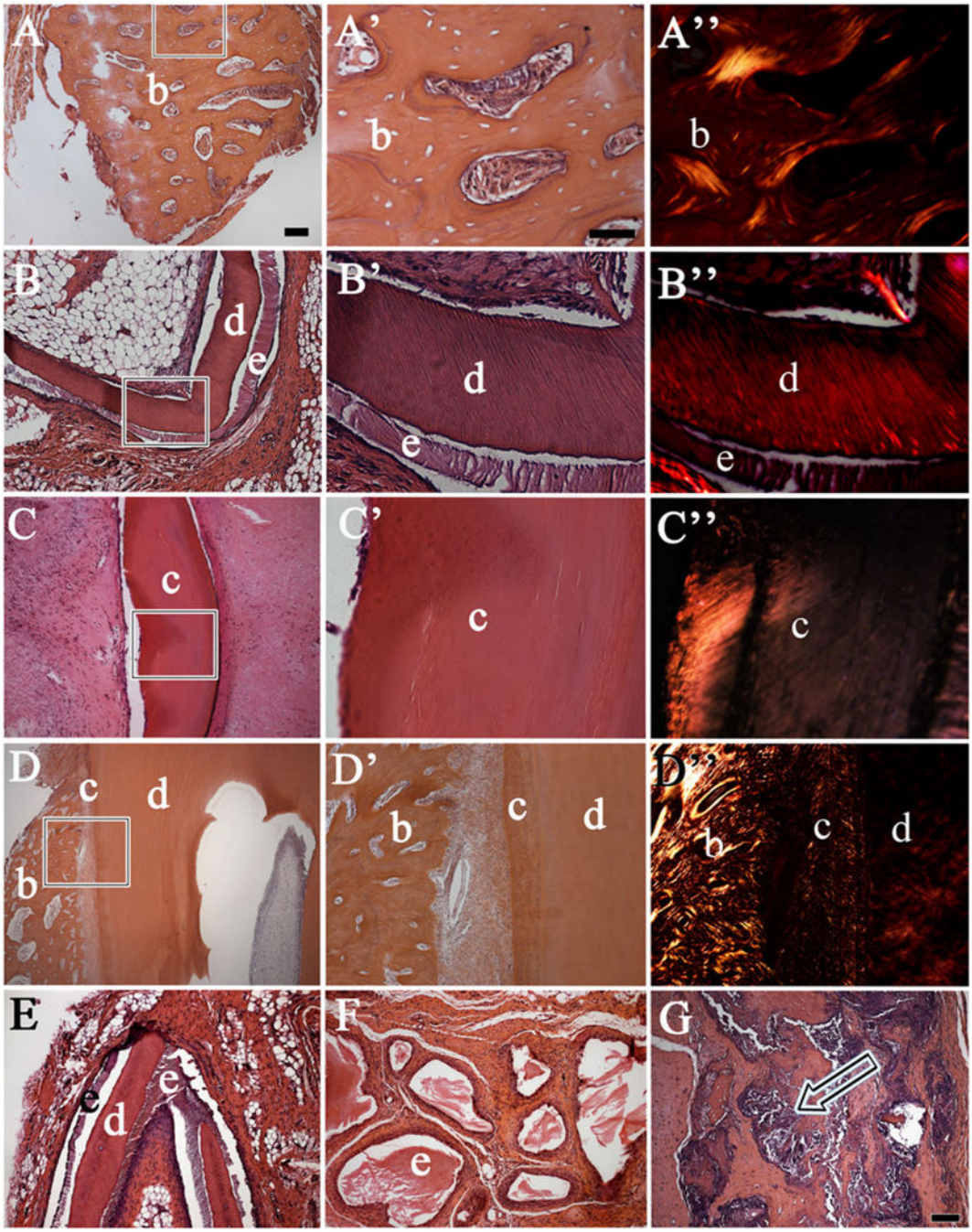

Figure 7.

Bioengineered mineralized tissue types. Letters with primes give higher magnification images of the boxed areas shown in the respective lettered panels. Haematoxylin and eosin (H&E) stained paraffin embedded and sectioned implant tissues revealed a variety of calcified recombinant tissues including (A,A') bone/osteodentin like tissue, (B,B') tooth crowns and (C,C') cementum tissue closely resembled that of naturally formed dental tissues (D,D'). Polarized light imaging revealed similar collagen fibre organization in bioengineered and natural mineralized tissues (A",B",C",D"). (E) A pDE-T + pDM-T recombinant

construct implanted subcutaneously for 1 month exhibited distinct sandwiched enamel–dentin–enamel tissue formation. (F) Demineralized enamel (e) present within a pDE-T + S recombinant construct. (G) Centrally located necrotic tissues with adjacent bone fragments present in M3 molar pDM-T + S construct (arrow). Abbreviations: b, bone; c, cementum; d, dentin; e, enamel; pDE-T, porcine dental epithelial tissue; pDM-T, porcine dental mesenchymal tissue; S, acellular collagen scaffold. Scale bars: 50 μm.

Table 1.

Summary of mineralized tissue formation in post-natal recombinant constructs

	Postnatal recombinant construct	Mineralized tissue types
1	pDE-T + pDM-T	9/12 (75%) Mineralized tissue formation 1/12 (8%) Tooth crowns with dentin and enamel
2	pDE-T + hDM-C	6/12 (50%) Mineralized tissue formation 1/12 (8%) Tooth crowns with dentin and enamel 12/12 (100%) Enamel matrix
3	pDE-T + S	6/12 (50%) Mineralized tissue formation 1/12 (8%) Tooth crowns with dentin and enamel 12/12 (100%) Enamel matrix
4	pDE-C + pDM-C	2/12 (17%) Mineralized tissue formation 1/12 (9%) Tooth crowns with dentin and enamel
5	hGE-C + hDM-C	1/12 (8%) Mineralized tissue formation
6	hGE-C + pDM-T	1/12 (8%) Mineralized tissue formation
7	pDM-T + S	0/12 (0%) Mineralized tissue formation

hDM-C, human dental pulp-derived dental mesenchymal cells; hGE-C, human gingival epithelial cells; pDE-C, porcine dental epithelial cells; pDM-C, porcine dental mesenchymal cells; pDM-T, porcine dental mesenchymal tissue; pDE-T, porcine dental epithelial tissue; S, acellular collagen scaffold.